Friction dependence of shallow granular flows from discrete particle simulations

Anthony Thornton[1,2,†], Thomas Weinhart[1,2], Stefan Luding[1] and Onno Bokhove[2]

[1] *Multi-Scale Mechanics, Dept. of Mechanical Engineering, Univ. of Twente, The Netherlands*
[2] *Numerical Analysis and Computational Mechanics, Dept. of Appl. Mathematics, Univ. of Twente, The Netherlands*
[†] *P.O. Box 217, 7500 AE Enschede, The Netherlands, Tel.: +31 53 489 3301, Fax: +31 53 489 4833, a.r.thornton@utwente.nl*

PACS 47.57.Gc – Complex fluids and colloidal systems: Granular flow
PACS 45.70.Ht – Granular systems: Avalanches
PACS 83.80.Fg – Rheology: Granular solids

Abstract – A shallow-layer model for granular flows is completed with a closure relation for the macroscopic bed friction or basal roughness obtained from micro-scale discrete particle simulations of steady flows. We systematically vary the bed friction by changing the contact friction coefficient between basal and flowing particles, while the base remains geometrically rough. By simulating steady uniform flow over a wide parameter range, we obtain a friction law that is a function of both flow and bed variables. Surprisingly, we find that the macroscopic bed friction is only weakly dependent on the contact friction of bed particles and predominantly determined by the properties of the flowing particles.

Memorandum 1958 (October 2011). ISSN 1874-4850. Available from: http://www.math.utwente.nl/publications
Department of Applied Mathematics, University of Twente, Enschede, The Netherlands

INTRODUCTION. – Free-surface flows of granular material occur in many geophysical and engineering applications, such as rockslides, avalanches, or production-line transport. They have been studied extensively both experimentally and numerically. The most direct way to simulate granular flows is by methods such as the Discrete Particle Method (DPM), which computes the movement of individual particles based on a model of the contact forces between the particles [1, 2]. However, realistic flow situations often involve billions of particles, and can only be modeled on a coarser level by continuum solvers (or hybrid methods), in which the particulate flow is described by a small number of continuum fields governed by the conservation of mass, momentum, and often energy. For shallow flows, the mass and momentum conservation equations can be further simplified by averaging over the flow depth, yielding granular shallow-layer equations [3–5]. In order to obtain a closed system of equations, closure relations for first normal stress ratio, velocity shape factor, and macro basal friction, have to be developed in terms of the flow variables: height, h and the depth-averaged velocity, $\bar{\boldsymbol{u}} = (\bar{u}, \bar{v})$. While closure models are usually developed to retain the qualitative behaviour of the microscopic system, they often cannot describe the quantitative behaviour as the relations between the micro- and macroscopic quantities are not well known.

Here, we focus on one closure relation: the effective macro-friction coefficient $\mu = \mu(h, |\bar{\boldsymbol{u}}|)$ and its dependence on the bed friction. It is informative to make a note about the nomenclature used in this paper. In the literature, the word friction gets used to mean both the macroscopic frictional forces felt by a large mass of material moving over a surface, as well as the contact frictional force between two individual flow particles, *i.e.,* the contact friction used in the DPM contact model. In this paper we will refer to the macroscopic (shallow-layer) friction as μ, and use μ^f for the particle-particle contact friction between flowing particles. There is one final complication: we will take a different value for the contact friction for contacts between flowing and base particles; this will be named μ^b.

The effective macro-friction coefficient, μ, determines the range of inclinations and heights at which the flow either arrests, reaches steady flow, or accelerates indefinitely. The rougher the base, the larger the range of inclinations at which steady flow is reached. Basal roughness can be modeled in various ways: in [6], a basal roughness was created by glueing particles onto a flat base. The roughness was changed by varying the diameter ratio between fixed basal and free flowing particles. They observed a peak in measured macro-friction coefficient at

a certain diameter ratio depending on the compactness of the basal layer. In their work on enduring contacts, Louge and Keast [7] modeled the basal roughness by assuming a flat frictional incline. Later, Louge [8] extended their theory to bumpy inclines. Silbert *et al.* [9] used DPM to simulate chute flow over a base of disordered particles. In [10], the effect of different basal types was investigated and they found that for a base of ordered particles the steady-state regime splits into three distinct flow regimes.

In our research we aim to obtain the closure relationships by studying small steady-state DPM simulations. First, a statistical method was developed [11] to extract the continuum fields from the microscopic degrees of freedom that is valid near the base of the flow. Then, an extensive parameter study was undertaken in [12] to study the full set of closure laws for the shallow water equations. Here, we extend the closure relation for the macro-friction coefficient by systemically changing the contact friction between basal and flowing particles, μ_b.

MATHEMATICAL BACKGROUND. –

Shallow layer model. The granular shallow-layer equations have proved to be a successful tool in predicting both geological large-scale [13–17] and laboratory-scale experiments [4, 18–20] of granular chute flows. They have been derived in many papers, starting with [3], but here we use the form presented in [4,5]. Shallow-layer theories assume that the flow is incompressible, the stress is isotropic and the velocity profile is uniform in depth. We will consider the flow down a slope with inclination θ with the x-axis downslope, y-axis across the slope and the z-axis normal to the slope. The free-surface and base location will be given by $z = s(x, y)$ and $z = b(x, y)$, respectively. The height of the flow is $h = s - b$ and velocity components are $\boldsymbol{u} = (u, v, w)^T$. Depth-averaging the remaining equations and retaining only high-order terms (in the ratio of height to length of the flow) yields the depth-averaged shallow-layer equations, *e.g.,* [4],

$$\frac{\partial h}{\partial t} + \frac{\partial}{\partial x}\left(h\bar{u}\right) + \frac{\partial}{\partial y}\left(h\bar{v}\right) = 0, \tag{1a}$$

$$\frac{\partial}{\partial t}\left(h\bar{u}\right) + \frac{\partial}{\partial x}\left(h\bar{u}^2 + \frac{g}{2}h^2\cos\theta\right) + \frac{\partial}{\partial y}\left(h\bar{u}\bar{v}\right) = S_x, \tag{1b}$$

$$\frac{\partial}{\partial t}\left(h\bar{v}\right) + \frac{\partial}{\partial x}\left(h\bar{u}\bar{v}\right) + \frac{\partial}{\partial y}\left(h\bar{v}^2 + \frac{g}{2}h^2\cos\theta\right) = S_y, \tag{1c}$$

where g is the gravitational acceleration, $\bar{\boldsymbol{u}} = (\bar{u}, \bar{v})$ the depth-average velocity and the source terms are given by

$$S_x = gh\cos\theta\left(\tan\theta - \mu\frac{\bar{u}}{\sqrt{\bar{u}^2 + \bar{v}^2}}\right)$$

and

$$S_y = gh\cos\theta\left(-\mu\frac{\bar{v}}{\sqrt{\bar{u}^2 + \bar{v}^2}}\right).$$

Here, for simplicity it has been assumed that b is constant. We note that various assumptions can be relaxed by introducing closure relations for the mean density, the normal stress ratio, and the shape of the velocity profile. This, however, is beyond the scope of this paper; we refer the interested reader to [12].

Friction law for rough surfaces. The closure to eqs. (1) is achieved by determining the bed macro-friction in terms of the flow variables, such that $\mu = \mu(h, |\bar{\boldsymbol{u}}|)$. In the early models a constant friction coefficient was used [3, 21], *i.e.,* $\mu = \tan\delta$, where δ is a fixed slope angle. For these models, steady uniform flow is only possible at a single inclination, δ, below which the flow arrests, and above which the flow accelerates indefinitely. However, detailed experimental investigations [22–24] for the flow over rough uniform beds show that steady flow emerges at a range of inclinations, $\delta_1 < \theta < \delta_2$, where δ_1 is the minimum angle required for flow, δ_2 is the maximum angle at which steady uniform flow is possible. In [23], the measured height $h_{stop}(\theta)$ of stationary material left behind when a flowing layer has been brought to rest, was fitted to

$$\frac{h_{stop}(\theta)}{Ad} = \frac{\tan(\delta_2) - \tan(\theta)}{\tan(\theta) - \tan(\delta_1)}, \quad \delta_1 < \theta < \delta_2, \tag{2}$$

where d is the particle diameter and A is a characteristic dimensionless length scale over which the friction varies. Here, we will investigate how the parameters A, δ_1 and δ_2 change as a function of the contact friction between bed and flowing particles.

For $h > h_{stop}$, steady flow exists where the Froude number, $F = |\bar{\boldsymbol{u}}|/\sqrt{gh\cos\theta}$, is assumed to fit a linear function of the height,

$$F = \frac{\beta h}{h_{stop}(\theta)} - \gamma\,, \; \delta_1 < \theta < \delta_2, \tag{3}$$

where β, γ are constants independent of the chute inclination and particle size.

From eqs. (2) and (3) we can derive a relation between the inclination θ and the flow variables F and h. For steady flow over a uniform bed, the momentum eqs. (1) reduce to $\mu = \tan\theta$, and by combining this with (2) and (3) we can derive the friction law

$$\mu(h, F) = \tan(\delta_1) + \frac{\tan(\delta_2) - \tan(\delta_1)}{\beta h/(Ad(F + \gamma)) + 1}. \tag{4}$$

Even though (4) is derived for steady-flow conditions it is expected to hold, in an asymptotic sense, for unsteady situations; therefore, it can be used as a closure relation for (1).

PROBLEM DESCRIPTION. –

Contact description. The DPM is used to perform simulations of a collection of mono-dispersed spherical granular particles of diameter d and density ρ_p; each particle i has a position $\boldsymbol{r}_i$, velocity $\boldsymbol{v}_i$ and angular velocity $\boldsymbol{\omega}_i$. It is assumed that particles are soft and have a single contact point. The relative distance is $r_{ij} = |\boldsymbol{r}_i - \boldsymbol{r}_j|$, the unit normal $\hat{\boldsymbol{n}}_{ij} = (\boldsymbol{r}_i - \boldsymbol{r}_j)/r_{ij}$ and the relative velocity $\boldsymbol{v}_{ij} = \boldsymbol{v}_i - \boldsymbol{v}_j$. Two particles are in contact if their

overlap, $\delta_{ij}^n = \max(0, d - r_{ij})$, is positive. The normal and tangential relative velocities at the contact point are given by

$$\boldsymbol{v}_{ij}^n = (\boldsymbol{v}_{ij} \cdot \hat{\boldsymbol{n}}_{ij})\hat{\boldsymbol{n}}_{ij}, \tag{5a}$$

$$\boldsymbol{v}_{ij}^t = \boldsymbol{v}_{ij} - (\boldsymbol{v}_{ij} \cdot \hat{\boldsymbol{n}}_{ij})\hat{\boldsymbol{n}}_{ij} + \frac{d - \delta_{ij}^n}{2}\hat{\boldsymbol{n}}_{ij} \times (\boldsymbol{\omega}_i + \boldsymbol{\omega}_j). \tag{5b}$$

Particles are assumed to be linearly viscoelastic; therefore, the normal and tangential forces are modeled as a spring-dashpot with linear elastic and linear dissipative contributions. Hence

$$\boldsymbol{f}_{ij}^n = k^n \delta_{ij}^n \hat{\boldsymbol{n}}_{ij} - \gamma^n \boldsymbol{v}_{ij}^n, \quad \boldsymbol{f}_{ij}^t = -k^t \boldsymbol{\delta}_{ij}^t - \gamma^t \boldsymbol{v}_{ij}^t, \tag{6}$$

with spring constants k^n, k^t and damping coefficients γ^n, γ^t; the elastic tangential displacement, $\boldsymbol{\delta}_{ij}^t$, is defined to be zero at the initial time of contact, and its rate of change is given by

$$\frac{d}{dt}\boldsymbol{\delta}_{ij}^t = \boldsymbol{v}_{ij}^t - r_{ij}^{-1}(\boldsymbol{\delta}_{ij}^t \cdot \boldsymbol{v}_{ij})\boldsymbol{n}_{ij}. \tag{7}$$

When the tangential-to-normal force ratio becomes larger than the contact friction coefficient, μ^c, the tangential spring yields and the particles slide, and we truncate the magnitude of $\boldsymbol{\delta}_{ij}^t$ as necessary to satisfy $|\boldsymbol{f}_{ij}^t| \leq \mu^c |\boldsymbol{f}_{ij}^n|$. Here $\mu^c = \mu^f$ for contacts between two flowing particles and μ^b for contacts between flow and basal particles. For more details on the contact law used in these simulations we refer the reader to [12]; whereas, in [2] a more complete discussion of contact laws, in general, can be found.

The total force on particle i is a combination of the contact forces $\boldsymbol{f}_{ij}^n + \boldsymbol{f}_{ij}^t$ between two particles i, j in contact and external forces, which for this investigation will be limited to gravity, $m\boldsymbol{g}$. We integrate the resulting force and torque relations in time using Velocity-Verlet and forward Euler [25] with a time step $\Delta t = t_c/50$, where t_c is the collision time [2]. The fixed bed particles are modeled as having an infinite mass and are unaffected by body and contact forces: they do not move.

In the following simulations, parameters are nondimensionalised such that the flow particle diameter $d = 1$, mass $m = 1$ and the magnitude of gravity $g = 1$. The normal spring and damping constants are $k^n = 2{\cdot}10^5$ and $\gamma^n = 50$; thus the contact duration is $t_c = 0.005$ and the coefficient of restitution is $\epsilon = 0.88$. The tangential spring and damping constants are $k^t = (2/7)k^n$ and $\gamma^t = \gamma^n$; hence, the frequency of normal and tangential contact oscillation and the normal and tangential dissipation are equal. These parameters are identical to those used by Silbert et al. [9] except that a dissipation in the tangential direction, γ^t, was added to dampen rotational degrees of freedom in arresting flow. In this investigation, the friction between bed and flowing particles, μ^b, is varied between $\mu^b = 0$ and ∞.

Chute geometry. DPM simulations are used to simulate uniform granular chute flows. The chute is periodic and of size 20×10 in the x- and y-directions, with inclination θ. The base is created by performing a 12 particle deep simulation of particles, across a flat surface, relaxing the system and then taking a cross-section to use as a rough bottom. More details of the base creation process can be found in [12].

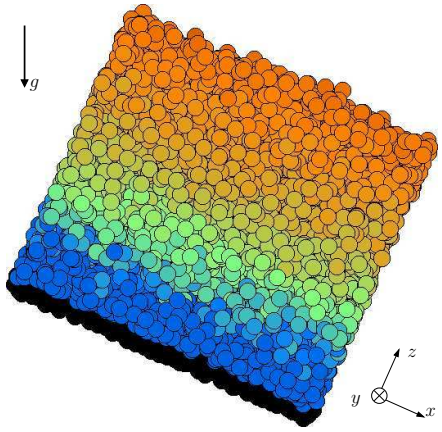

Fig. 1: DPM simulation for $N = 3500$, inclination $\theta = 24°$ and the basal contact friction, $\mu^b = 0.5$, at time $t = 2000$; gravity direction $\boldsymbol{g}$ as indicated. The domain is periodic in the x- and y-directions. In the plane normal to the z-direction, fixed (black) particles form a rough base while the surface is unconstrained. Colours indicate speed, which increase from slow (blue) at the bottom to faster (orange) towards the free-surface.

The height of the flow is determined by the number of flow particles, N, which are initially randomly distributed with a low packing fraction of about $\rho/\rho_p = 0.3$. From this state the particles collapse and compact to a height of approximately, $N/200$, giving the chute enough kinetic energy to initialise flow. Time is integrated from $t = 0$ to $t = 2000$ (20 million time steps) to allow the system to reach steady state. A screen shot of a system in steady state is given in fig. 1.

Statistics. To obtain macroscopic fields from the DPM simulations, we use the coarse-graining statistical methods as described in [26, 27], extended to incorporate external boundary forces [11]. For coarse-graining a course-graining function, that spatially smears the discrete data has to be defined; we use a Gaussian of width, or variance, $d/4$.

The flow is assumed steady at $t = 2000$ if the kinetic energy has been constant over the interval $1500 < t < 2000$. To obtain depth profiles of the macroscopic fields in steady state, an average is taken over $t \in [2000, 2100]$ and the x and y directions. The height of the flow is defined to be the distance between the point where the downwards normal stress σ_{zz} vanishes and where it reaches its maximum value. In order to avoid the effects of coarse graining, we used the height where the stress was 1% and 99% of the maximum stress; then we linearly extrapolated the bulk stress profile to define the base and surface locations (see

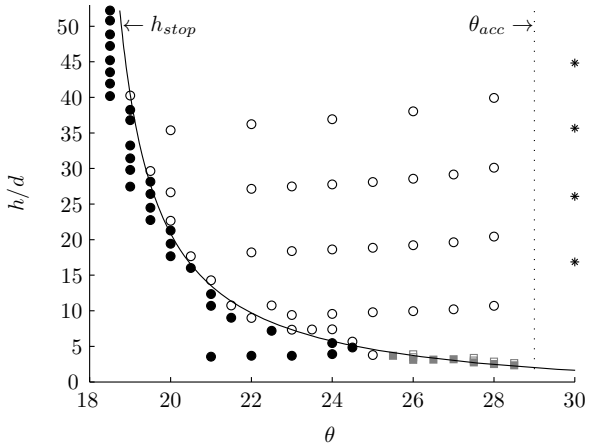

Fig. 2: Overview of DPM simulations for $\mu^b = 0.5$, with markers denoting the state: arrested filled-symbols, steady open-symbols, and accelerating $*$. The demarcation line is fitted to h_{stop} in eq. (2) (solid line). Note, circular symbols are for increasing the number of particles and square symbols for decreasing.

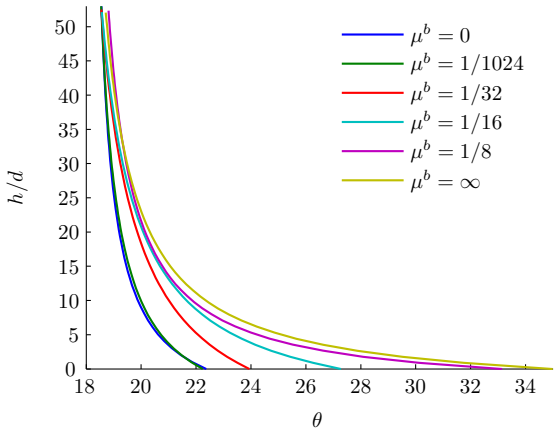

Fig. 3: Demarcation lines $h_{stop}(\theta;\mu^b)$ between retarding and steady flows for various values of μ^b. The demarcation line is fitted to eq. (2).

[12] for details).

RESULTS. –

The steady flow regime. From the experiments of Pouliquen [22], steady granular flow over a rough base is known to exist for a range of heights and inclinations, $\theta_{stop}(h) < \theta < \theta_{acc}$, where $\theta_{stop}(h)$ denotes the inverse function of $h_{stop}(\theta)$. The range of steady flow was previously determined using DPM simulations by [9]. However, the simulations provided too few data points near the boundary of arrested and steady flow to allow a fit of the stopping height.

To determine the demarcation line between arrested and steady flow with good accuracy (the h_{stop}-curve), a set of simulations were performed with initial conditions determined by the following algorithm: Starting with $N = 1000$ flow particles and inclination $\theta = 21°$, the angle was increased in steps of $1°$ until a flowing state was reached. If the flow arrested, the number of particles was increased by $N = 400$ or else the angle decreased by $1/2°$. Flow was defined to be arrested when the ratio between kinetic energy and the elastic energy stored in the contact, E_{kin}/E_{ela}, fell below 10^{-5} before $t = 500$ was reached, otherwise the flow was determined as flowing. In contrast to [12], we also determined the demarkation line for thin flows: Starting with $N = 1000$, the angle was increased by $1/2°$, if the flow arrested; otherwise the number of particles was decreased by 10% until $N < 200$ was reached. Note, these simulations are shorter than the ones used to determine the flow properties, due to the large number of simulations required to obtain high resolution h_{stop}-curves. Thus, we obtain inclination intervals at various heights and height intervals at various inclinations between which the actual demarcation line lies, see fig. 2. The demarcating curve was then fitted to eq. (2) by minimising the distance of the fit to these intervals. The observed fittings are illustrated in fig. 4.

A general friction law. First, we study the effect of basal contact friction on the range of steady flows, μ^b. This yields a family of demarcation curves between arrested and steady states, $h_{stop}(\theta;\mu^b)$, which can all be fitted to the Pouliquen h_{stop}-curve (2). In order to obtain a function for the bed macro-friction, we used the approach of Pouliquen who found that for rough bases the Froude number is a linear function of $h/h_{stop}(\theta)$. Our first approach was to fit the Froude number to $h/h_{stop}(\theta;\mu^b)$; however, it was found that a better collapse is obtained if the Froude number is fitted with the h_{stop}–curve for the case where the flowing and base particles are identical, *i.e.*, $\mu^f = \mu^b$ such that

$$F = \beta(\mu^b)\frac{h}{h_{stop}(\theta;\mu^f)} - \gamma(\mu^b), \qquad \theta_{stop}(h;\mu^b) \le \theta \le \theta_{acc}(\mu^b), \tag{8}$$

for all steady flows. This modification to h_{stop} is a key finding.

The fits to these curves are shown in fig. 3; the fitting parameters $\delta_1(\mu^b), \delta_2(\mu^b)$ and $A(\mu^b)$ can be found in fig. 4. The value of δ_1 shows no sensitivity to μ^b, which is to be expected as δ_1 is strongly related to the angle of repose of material, which is not a function of the base configuration. For, $\mu^b \le 1/4$, δ_2 decreases as μ^b is decreasing; whereas A increases, resulting in a net reduction in the effective macro-friction coefficient, μ, as is clearly illustrated in fig. 3.

When plotting h/h_{stop} versus the Froude, $h_{stop}(\theta;\mu^f)$ was used instead of $h_{stop}(\theta;\mu^b)$ because it gives a better collapse and is defined for all inclinations for which steady flow exists. The proportionality constant, β, and offset, γ, are shown in fig. 5 and again appear almost independent of μ^b. In the case $\mu^b = 0$ there is a sharp reduction in γ, even compared to $\mu^b = 1/1024$, implying a change in

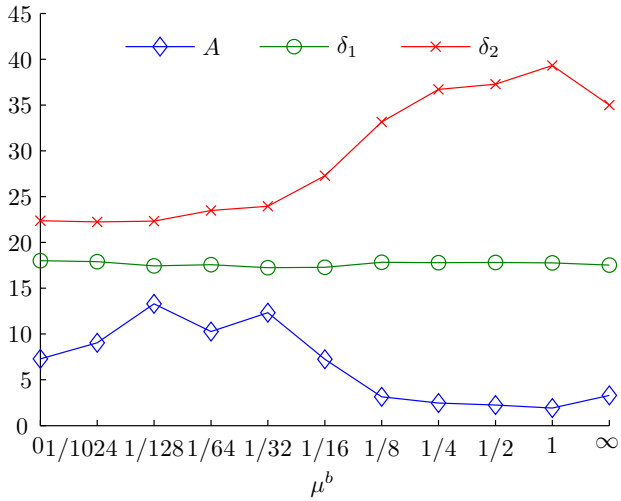

Fig. 4: Figure showing how A, δ_1 and δ_2 depend on the contact friction coefficient between base and flowing particles, μ^b.

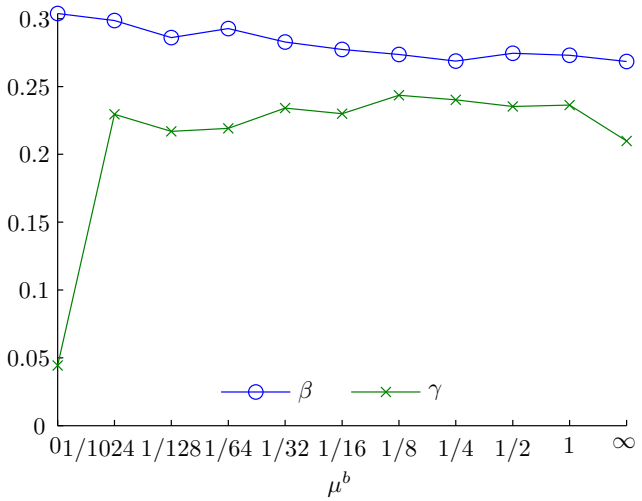

Fig. 5: Figure showing the dependence of β and γ on the contact friction coefficient between base and flowing particles μ^b.

the flowing behaviour when the contact friction is 'turned off'. Thus, the friction coefficient of the depth-averaged eqs. (1) is given by

$$\mu(h, F; \mu^b) = \tan(\hat{\delta}_1) + \frac{\tan(\hat{\delta}_2) - \tan(\hat{\delta}_1)}{\frac{\beta(\mu_b)h}{Ad(F+\gamma(\mu_b))} + 1},$$
$$\theta_{stop}(h; \mu^b) \leq \tan^{-1}\mu \leq \theta_{acc}(\mu^b), \qquad (9)$$

where the hat denotes *e.g.,* $\hat{\delta^1} = \delta^1(\mu^f)$, etc. The values obtained for the parameters are given in figs. 4 and 5. The key results are that the only dependence of the macro-friction, μ, on the bed contact friction, μ^b, is through the coefficients β and γ, *i.e.,* (9) is valid for all steady flows, for beds with varying micro friction, and only β and γ are functions of μ^b, all other parameters are determined by μ^f. A detailed investigation of how A, δ^1 and δ^2 depend on other flow parameters has been undertaken in [12].

Frictional dependence in the depth profiles. For all simulations we observe nearly constant, with depth, density profiles, and linear stress profiles for σ_{xx} and σ_{xz}, which satisfy the mass and momentum balances for steady uniform flow. Additionally, we do find a normal stress anisotropy, *i.e.,* $\sigma_{xx} \neq \sigma_{zz}$. Fig. 6 shows a selection of velocity profiles. We observe a Bagnold profile as predicted in [28] for thick collisional flows. A small deviation from the Bagnold profile is observed at the surface, where the profile becomes linear and near the base where the shear rate decreases. For $\mu^b = 0$, the flow shows a slip velocity at the base, a characteristic of smoother flows and is not observed for the case $\mu^b = 1/1024$. This implies a sharp change in the flow behaviour near the base when the basal contact friction is included in the particle contact model. Combined with a similar 'discontinous' change in γ between $\mu^b = 0$ and $\mu^b \neq 0$ it appears there is a fundamental change in the flow characteristics when a basal contact friction is added to the DPM model. However, the mean density and the shape of the velocity profile both show a dependence on the inclination and height of the flow [12].

CONCLUSIONS. – A closure relation for the macroscopic basal friction in a shallow-layer model of granular flow, over a geometrically rough bed, was obtained using DPM simulations. An extensive parameter study of steady uniform flows was undertaken by varying height h, inclination θ and the basal contact friction μ^b. At small inclinations, the flow quickly retards and a static pile is formed; at large inclinations, the flow continued to accelerate; between these two regimes there was a range of inclinations at which steady flows were observed, see fig. 2. Depth profiles for density, velocity and stress were measured using coarse-grained macroscopic fields. A novel definition of the stress at the boundary was used cf. [11], which exactly satisfies the mass and momentum balance, even near the boundary. The assumptions of depth-averaged theory are found to be valid for steady uniform flow: the density is almost constant in depth, and the downward normal and shear stress balances the gravitational forces acting on the flow (both local and in depth-averaged form).

The results of the DPM simulations did not vary significantly with the contact friction at the bed; variations were only observed for small values of the basal contact friction, $\mu^b < 1/4$. For small values of μ^b the demarcation curves $h_{stop}(\theta; \mu^b)$, $\theta_{acc}(\mu^b)$ between arrested, steady and accelerating flows shifted to the left, see fig. 3, implying a lower macro-friction coefficient, μ. Thus, a steady state was observed at smaller inclinations and heights. For the special case of $\mu^b = 0$, the flow developed a small slip velocity at the base, see fig. 6. Additionally, the offset in the dependance of height on Froude number sharply changed between the case $\mu^b = 0$ and $\mu^b \neq 0$, indicating a change in the flow characteristics, when basal contact friction is added to the contact model.

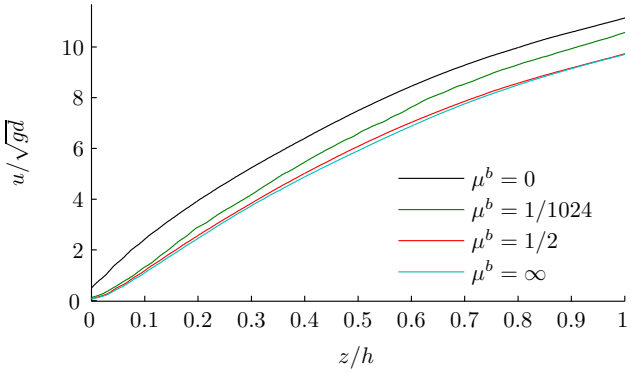

Fig. 6: Flow velocity profile for thick flow with $N = 6000$ ($H = 30$), inclination $\theta = 24^\circ$ and bed micro-friction $\mu^b = 0, 1/1024, 1/2, \infty$. The flow velocity roughly observes a Bagnold profile, except near the surface and the base. For $\mu^b = 0$ the flow shows a slip velocity at the base.

The bed friction, $\mu = \tan\theta$, was expressed as a function of height and flow velocity, cf. (9). This was done by extending the approach of Pouliquen for varying contact friction at the bed: the Froude number is a linear function of $h/h_{stop}(\theta;\mu^f)$, *i.e.,* the stopping height is determined by the flowing, not the basal, particles. The results in this paper suggest that macroscopic closure relations for shallow granular flow can be expressed in terms of the microscopic parameters. This approach yields the closure relation for the friction coefficient for the shallow-layer continuum model allowing large-scale computations (*e.g.,* [29]) of granular flows using continuum equations.

The friction law developed here is strictly only valid for steady flows of mono-dispersed particles for the established inclination range $\theta_{stop}(h;\mu^b) \leq \tan^{-1}\mu \leq \theta_{acc}(\mu^b)$. However, it is anticipated, that it will still hold for slightly poly-dispersed particles, slowly varying basal properties, and across a wider range of angles. The exact range of applicability of the closure law still has be determined and this will form the theme of future work.

Both the results presented here and in [12], where the geometric basal roughness (size of basal particles) was changed, show that the flow rule for the case where bed and flow particles are the same gives the best collapse. Therefore, for the macroscopic friction coefficient, μ, the main result of these studies is: The only dependence of μ on the base properties is through the relationship of the Froude number against $h_{stop}(\theta;\mu^f)$. In other words, the macroscopic friction coefficient, μ is mainly determined by the properties of flowing material and, hence, the Pouliquen law may still give insight for flows over smooth surfaces, where at the moment it is thought to be of limited applicability.

REFERENCES

[1] Cundall P. and Strack O., *Geotechnique*, **29** (1979) 47.
[2] Luding S., *European J. of Environ. Civil Eng.*, **12** (2008) 785.
[3] Savage S. and Hutter K., *J. Fluid Mech.*, **199** (1989) 177.
[4] Gray J., Tai Y. and Noelle S., *J. Fluid Mech.*, **491** (2003) 161.
[5] Bokhove O. and Thornton A., *Shallow granular flows* in *Handbook of Environmental Fluid Dynamics*, edited by Fernando H., (CRC Press) 2012.
[6] Goujon C., Thomas N. and Dalloz-Dubrujeaud B., *Eur. Phys. J. E*, **11** (2003) 147.
[7] Louge M. and Keast S., *Phys. Fluids*, **13** (2001) 1213.
[8] Louge M., *Phys. Rev. E*, **67** (2003) 061303.
[9] Silbert L., Ertas D., Grest G., Halsey, T.C. Levine D. and Plimpton S., *Phys. Rev. E.*, **64** (2001) 051302.
[10] Silbert L., Grest G., Plimpton S. and Landry J., *Phys. Fluids*, **14** (2002) 2637.
[11] Weinhart T., Thornton A., Luding S. and Bokhove O., *Granular Matter*, submitted, special volume for Goldhirsch (2011) .
[12] Weinhart T., Thornton A., Luding S. and Bokhove O., *Granular Matter*, submitted (2011) .
[13] Cui X., Gray J. and Johannesson T., *J. Geophys. Res.*, **112** (2007) F04012.
[14] Doyle E., Hogg A., Mader H. and Sparks R., *Geophys. Res. Lett.*, **35** (2008) L04305.
[15] Denlinger R. and Iverson R., *J. Geophys Res.*, **106** (2001) 533.
[16] Dalbey K., Patra A., Pitman E., Bursik M. and Sheridan M., *J. Geophys. Res.*, **113** (2008) B05203.
[17] Williams R., Stinton A. and Sheridan M., *J. Volcan. Geotherm. Res.*, **177** (2008) 760.
[18] Hákonardóttir K. and Hogg A., *Phys. Fluids*, **17** (2005) 077101.
[19] Gray J. and Cui X., *J. Fluid Mech.*, **579** (2007) 113.
[20] Vreman A., Al-Tarazi M., Kuipers A., Van Sint Annaland M. and Bokhove O., *J. Fluid Mech.*, **578** (2007) 233.
[21] Hungr O. and Morgenstern N., *Geotechnique*, **34** (1984) 415.
[22] Pouliquen O., *Phys. Fluids*, **11** (1999) 542.
[23] Forterre Y. and Pouliquen O., *J. Fluid Mech.*, **486** (2003) 21.
[24] GDR MiDi, *Eur. Phys. J. E.*, **14** (2004) 341.
[25] Allen M. and Tildesley D., (Editors) *Computer Simulation of Liquids* (Oxford University Press) 1993.
[26] Babic M., *Int. J. Eng. Science*, **35** (1997) 523 .
[27] Goldhirsch I., *Granular Matter*, **12** (2010) 239.
[28] Bagnold R., *Proc. Roy. Soc. A*, **255** (1954) 49.
[29] Pesch L., Bell A., Sollie W., Ambati V., Bokhove O. and Van der Vegt J., *ACM Transactions on Mathematical Software*, **33** (2007) 4.

* * *

The authors would like to thank the Institute of Mechanics, Processes and Control, Twente (IMPACT) for its financial support.